Hydrolysis of the Prodrug, 2',3',5'-Triacetyl-6-azauridine

C. M. Riley,[1,4] M. A. Mummert,[1] J. Zhou,[1]
R. L. Schowen,[1] D. G. Vander Velde,[1,2]
M. D. Morton,[2] and M. Slavik[1,3]

Received December 19, 1994; accepted March 24, 1995

Purpose. The purposes were to study the kinetics of hydrolysis of 2',3',5'-triacetyl-6-azauridine (*1*) in aqueous solution (μ = 0.5) and to identify the main intermediates and products of the reaction. ***Methods.*** A stability indicating isocratic LC assay was used to study the rate of degradation of *1*. A gradient LC assay was used to study the time courses of the degradants. The products of hydrolysis were isolated by preparative liquid chromatography and identified by ^{1}H-NMR and CI-MS. The pK_a value was obtained by potentiometric titration. ***Results.*** At 36.8°C, the pH-rate profile of *1* in water was adequately described by a four-term rate equation. The intermediates were identified as the primary and secondary di-acetates, and the primary and secondary mono-acetates. The final product was 6-azauridine. ***Conclusions.*** A simplified kinetic scheme could be used to describe the concentration-time profiles of *1*, the intermediates and the final product.

KEY WORDS: 2',3',5'-triacetyl-6-azauridine; prodrug; hydrolysis; pH-profile; arrhenius plots; CI-MS; NMR; liquid chromatography.

INTRODUCTION

2',3',5'-Triacetyl-6-azauridine (*1*) is an orally active prodrug of the anti-psoriasis and antineoplastic drug 6-azauridine (*2*). It is chemically and enzymatically deacylated to *2* and then metabolized to the nucleotide 5'-monophosphate, which inhibits the growth of neoplasms by inhibiting orotidine 5'-phosphate decarboxylase, *i.e.*, interfering with the ability of cells to utilize orotidine 5'-phosphate (1). This inhibition of growth is selective for neoplastic cells and has low toxicity to normal tissues. 6-Azauridine has also been shown to have antiviral activity (2). The active drug, *2*, itself is incompletely absorbed in the upper intestine and intestinal flora catabolize *2* to 6-azauracil, *3* (Figure 1), which has CNS toxicity. This latter side effect can be reversed by withdrawing treatment. The observation that intravenous injection of *2* itself causes no CNS toxicity (3) led to the synthesis of the prodrug *1*, which is completely absorbed in the upper intestine and concomitantly no CNS toxicity is observed with oral administration.

The antineoplastic effects of *2* as an antimetabolite have been demonstrated, frequently in combination with other drugs because of the moderate neoplastic effect and the mild side effects (4,5). The prodrug, *1*, was approved by the FDA in February 1975 under the generic name azaribine for the oral treatment of severe psoriasis but was recalled in August 1976 because it may cause life-threatening and potentially fatal blood clots in the veins and arteries. The clotting seemed to be drug-induced as most thromboembolic episodes occurred during the 6-week period of treatment (6). The toxicity was caused by the depletion of pyridoxal phosphate in the plasma by reaction with those catabolites of *2* which have an open triazine ring and make up about 5% of the degradation products of an IV-administered dose of *2* (6). This depletion is prevented by the addition of high doses of vitamin B-6 (6,7).

6-Azauridine itself is 95% excreted by the body in 8 h, and may be safely employed in man over long periods by IV injection of up to 600 mg/kg/24h. The prodrug, *1*, slowly deacetylates in serum, and generates high levels of *2* in the plasma for 8 hours after dosing (8). Most of an orally administered dose of *1* is excreted as *2*, with a portion excreted as the monoacetate and infrequently as the diacetate (2). There is little quantitative information in the literature on the hydrolysis of 2',3',5'-triacyl-prodrugs of nucleosides in general or on the hydrolysis of *1* in particular. Knowledge of the rates and mechanisms of degradation will help in the rational design of dosage forms as well providing the analytical and kinetic framework for the study of the enzymatic conversion of such prodrugs to their active forms. Particularly difficult challenges encountered in the present study on the chemical hydrolysis of *1* involved the development of an assay for the simultaneous analysis of *1*, *2*, and *3*, the three positional isomers of the diacetate (*4a*, *4b*, and *4c*), and the three positional isomers of the monoacetate (*5a*, *5b*, and *5c*); and the development of a manageable kinetic scheme to describe the time courses of the 9 compounds of interest.

MATERIALS AND METHODS

Materials

2',3',5'-Triacetyl-6-azauridine (Figure 1) was a gift from Dr. William Drell, U.R. Laboratories, La Jolla, CA. Samples of *2* and *3* were obtained from Sigma Chemical Co. (St. Louis, MO). All water was deionized with a Milli-Q Water System from the Millipore Corporation, Bedford, MA. Hydrochloric acid, phosphoric acid, acetic acid, sodium dihydrogen phosphate, disodium monohydrogen phosphate, sodium acetate, borax, dipotassium carbonate, potassium hydrogen carbonate, and sodium hydroxide were reagent grade and purchased from commercial sources. The sodium chloride used to adjust the ionic strength to 0.50, certified buffer solutions used to standardize the pH meter, and High Performance Liquid Chromatography (HPLC) grade methanol and acetonitrile were obtained from Fisher Scientific, St. Louis, MO. The 0.1052 M volumetric standard sodium hydroxide solution used for pK_a determinations was obtained from Aldrich Chemical Company, Milwaukee, WI.

[1] Department of Pharmaceutical Chemistry and the Center for Bio-Analytical Research, University of Kansas, Lawrence, KS 66045-2504, USA.
[2] NMR Laboratory, University of Kansas, Lawrence, KS 66045-2504, USA.
[3] Veterans Administration Center, 5500 E. Kellogg, Wichita KS 67218, USA.
[4] To whom correspondence should be addressed at Analytical Research and Development Department, DuPont Merck Pharmaceutical Company, P.O. Box 80400, Wilmington, DE 19880-0400, USA.

0724-8741/95/0900-1361$07.50/0

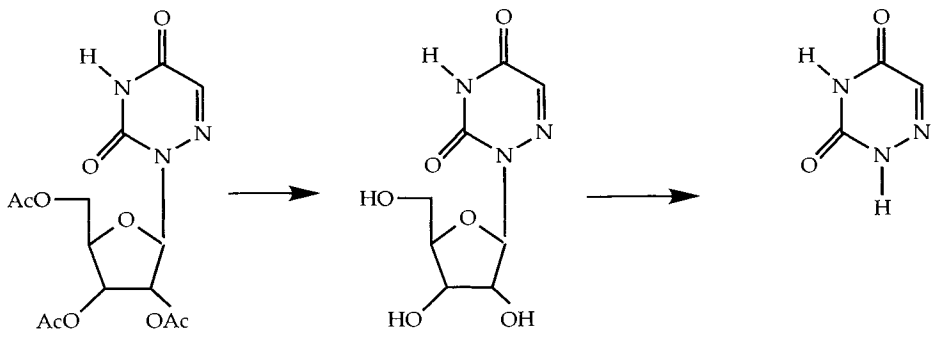

2',3',5'-Triacetyl-6-azauridine (1) 6-Azauridine (2) 6-Azauracil (3)

Fig. 1. Proposed bioconversion of the prodrug 2',3',5'-triacetyl-6-azauridine (*1*).

Methods

Kinetic Studies

The rate of degradation of *1* was determined at 36.8 ± 0.2°C over the range 1.00 to 9.93. The effect of both pH and temperature on the degradation of *1* was studied as follows: pH 2.06 (36.8, 50.0, 60.0, and 70.0°C), pH 4.51 (36.8, 50.0, 70.0, and 90.0°C), pH 7.51 (36.8, 50.0, 60.0, and 70.0°C). The following buffers were used to control the pH of the solutions: HCl (pH 1.00), phosphate (1.80–3.06, and 5.99–7.49), acetate (3.51–5.51), borate (8.00–9.50) and carbonate (9.00–9.93). Each buffer was studied at three concentrations (0.05, 0.10, and 0.15 M) and the ionic strength was adjusted to 0.5 with NaCl in all cases. Each buffer level was studied in duplicate and the data from both runs were used to calculate the rate constants. All pH measurements for the kinetic studies were made at the temperature of the experiments. The pH was measured at the beginning and at the end of the kinetic experiments. For all experiments the change in pH was less than 0.03. For kinetic studies that were complete within 10 h samples were stored in tightly capped 25 ml glass vials. For studies lasting more than 10 h, the samples were sealed in glass ampoules. Constant temperatures (±0.1°C) were maintained by either storing the samples in a constant temperature oven or by immersing in a constant temperature water bath.

Isocratic Liquid Chromatography

This technique was used to determine the rate of loss of *1* from aqueous solutions. The liquid chromatograph consisted of an Altex 110A pump (Beckman Instruments, Fullerton, CA), an Altex 210 injector fitted with a 20 μl loop, an Upchurch A.314 precolumn filter (Upchurch Scientific, Oak Harbor, WA), an ODS Hypersil guard column (10 × 4.6 mm, 5 μm), an ODS Hypersil analytical column (150 × 4.6 mm, 5 μm), a SpectroMonitor D variable wavelength UV detector, (LDC/Milton Roy, Riviera Beach, FL) and a Shimadzu C-R6A chromatopac integrator (Shimadzu Corporation, Kyoto, Japan). Samples (20 μl) were injected into the system by the overfill method, and the degradation of *1* was followed for at least 3 half-lives. The flow rate was 1.5 ml/min and UV detection was at 254 nm. Peak areas were used for quantification. The mobile phase was water/methanol (65:35 v/v) containing 0.05 M phosphate, with the pH of the aqueous components being 6.0. The mobile phase was filtered through a 0.22 μm nylon filter after preparation and degassed before use by helium sparging for 5 min. The linear range of the method for *1* was 0.5–150 μg/ml. Changes in detector response during the stability study were measured by assaying a standard sample of 100 μg/ml *1*, separated into 1 ml aliquots and frozen at −20°C. The standard solution was measured to determine the daily response of the detector. The variation in the detector response throughout the whole course of the study was less than 10%. Under these isocratic conditions, the parent compound, *1* eluted with a retention time of 3.0 min and its degradation products eluted at or close to the solvent front.

Gradient Elution Liquid Chromatography

This technique was used to separate *1* and eight apparent degradation products (*2*, *3*, *4a-c*, and *5a-c*) (Figure 2). The chromatograph consisted of two LKB 2150 pumps and an LKB 2152 controller (LKB-Produkter AB, Bromma, Sweden), an Omni helium sparging solvent delivery system (Omnifit Ltd., West Germany), an Altex 210 injector fitted with a 20 μl loop, an Upchurch A.314 precolumn filter (Upchurch Scientific, Oak Harbor, WA), either a SpectroMonitor D variable wavelength UV detector, (LDC/Milton Roy, Riviera Beach, FL) or a Perkin Elmer LC-235 diode array detector (Perkin Elmer Corporation, Norwalk, CT), a 100 psi backpressure regulator, and a Shimadzu C-R6A chromatopac integrator (Shimadzu Corporation, Kyoto, Japan). For the analytical separations 20 μL of sample was injected by the overfill method into an ODS Hypersil guard column (10 × 4.6 mm, 5 μm), connected to an ODS Hypersil analytical column (150 × 4.6 mm, 5 μm), and the appearance and disappearance of degradation products was followed over time. The flow rate was 1.0 ml/min. Solvent *A* was a phosphate buffer and mobile phase *B* was a phosphate buffer-acetonitrile (70:30 v/v) both phases being 0.05 M in phosphate and the pH of the aqueous components being 3.0. The gradient profile was 100% *A* for 5 min, ramping to 100% B at 25 min, then to 100% *A* at 26 min and re-equilibrating after 5 min. Helium sparging of both solvents was critical for a stable baseline. A representative chromatogram is shown in Figure 2.

The preparative chromatography system was the same

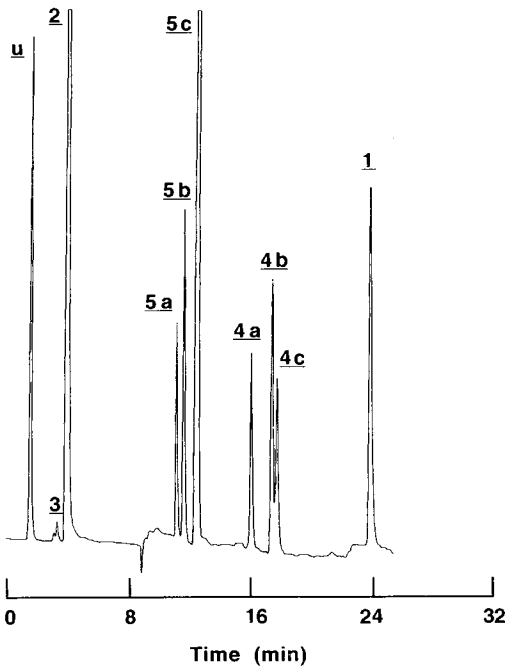

Fig. 2. Gradient separation of 2',3',5'-triacetyl-6-azauridine (*1*) from its degradation products (*2–5*). Stationary phase: ODS Hypersil (5 μm, 150 × 4.6 mm, i.d.), mobile phase: Solvent *A* phosphate buffer; Solvent *B* water-acetonitrile (70:30 v/v) both phases being 0.05 M in phosphate and the pH of the aqueous components being 3, flow rate: 1.0 ml/min, temperature: ambient, detection wavelength: 254 nm.

as the gradient elution system described above except a 50 cm Whatman Magnum 9 column packed with Partisil 10 ODS-2 and a 500 μl injection loop replaced the corresponding analytical scale components. Solvent *A* was a phosphate buffer-acetonitrile (5:95, v/v) and Solvent *B* was phosphate buffer/acetonitrile (50:50 v/v) both phases being 0.05 M in phosphate and the pH of the aqueous components being 3.0. The gradient profile was 100% *A* for 15 min, ramping to 15% *B* at 30 min, to 50% *B* at 35 min, to 100% *A* at 45 min, then 100% *A* at 46 min and re-equilibrating after 10 min. The flow rate was 4.5 ml/min and UV detection was at 254 nm. Under these conditions *1* and *2* eluted at 42.0 and 4.5 min, respectively.

pKa Determination

The pK_a of *1* was determined titrimetrically by the method of Albert and Serjeant (9) as follows: 6.42 ± 0.02 (25.0°C, μ = 0.00), 6.28 ± 0.06 (25.0°C, μ = 0.05), and 6.15 ± 0.04 (36.8°C, μ = 0.50). The pK_a values at μ = 0.00 were corrected for ionic strength. The temperature was regulated with a Fisher Scientific Model 900 constant temperature circulator. A combination pH electrode with calomel reference (Markson Scientific, Phoenix, AZ) was used to determine the pH, which was measured with a Corning 150 Ion Analyzer with a resolution of 0.001.

Data Analysis

The loss of *1* was pseudo first order in all cases. Pseudo first order rate constants (k_{obs}) were obtained by least squares linear regression analysis of the relationship relating the logarithm of the concentration of *1*, remaining ($[1]_t$) and time, *t* (Eq. 1):

$$\ln \frac{[1]_t}{[1]_o} = -k_{obs}t \quad (1)$$

where $[1]_o$ is the initial concentration of *1*. Data were fitted to non-linear equations using the program MINSQ® on a Compaq 384 personal computer or Deltagraph® Professional version 2.0 on Macintosh personal computers. Computer simulations were generated with a spreadsheet (MS Works®) and the plotted using Deltagraph® Professional version 2.0 on Macintosh personal computers.

Characterization of Degradation Products

The degradation products of *1* were collected by preparative liquid chromatography, and analyzed by mass spectrometry and high field ^{1}H-NMR. A 1.5 ml aliquot of partially degraded *1* was injected in 500 μl aliquots into the preparative LC system. Four fractions corresponding to the peaks eluting with retention times of 13.5 (fraction 1), 20.0 (fraction 2), 30.0 (fraction 3) and 34.5 min (fraction 4) were collected in 20 ml scintillation vials and frozen immediately. Subsequently, the aliquots were placed in a VirTis Bench Top 1.5 freeze drier (VirTis Company, Gardiner, NY) attached to a Cenco Hyvac 14 vacuum pump (Cenco Instruments Company, Chicago, IL) and lyophilized at a pressure of approximately 100 m Torr and an initial shelf temperature of −45°C. When the shelf temperature rose to 0°C after 48 h, the samples were removed and stored in a vacuum descicator at room temperature.

After reconstitution in water, chemical ionization (CI) mass spectra of the fractions were obtained on a Nermag (Paris, France) R10–10 quadrapole mass spectrometer equipped with a SPECTRAL 30 data system. Samples were desorbed from a heated wire in the ion volume using a heating current of 50mA/s programmed to 500 mA. The source temperature was 250°C, the emission current was 200 mA and 70eV electron energy was used. The quadrapole was scanned from 40–650 amu at 305 amu/sec. CI spectra were obtained with ammonia as the reagent gas at a source pressure previously optimized using perfluorotributylamine-derived ions.

The ^{1}H-NMR spectra of the intermediates were recorded at room temperature (22 ± 1°C) on a Bruker AM-500 NMR spectrometer. The solutions were prepared in D_2O and spectra were referenced to external TSP (3-(trimethylsilyl)propionic-2,2,3,3-d_4 acid).

RESULTS AND DISCUSSION

Loss of the Prodrug

Effect of Initial Concentration

The pseudo first-order rate constant of degradation of *1* was found to be independent of concentration at pH (μ = 0.50) and 36.8°C. This set of experiments also established that a minimum initial concentration of 10 μg/ml for *1* limited the error in the rate constant due to LC analysis to less than 0.2%. For this reason, initial concentrations of 10–20 μg/ml *1* were used in most kinetic experiments, with somewhat higher concentrations being used for degradations lasting less than 12 h.

Buffer Catalysis

Phosphate, acetate, and borate buffers catalyzed the degradation of *1* while carbonate had no catalytic effect. The values of the general catalysis constant, k_G, were plotted against the fraction of the more basic species (f_{base}) to obtain the catalytic rate constants for the individual buffer species (Figure 3, Table I) Two values for $k_{H_2PO_4^-}$ were obtained, one at pH 1.80–3.06 and another at pH 5.99–7.49. The latter value was determined in a pH range that encompasses a pK_a for *1*, and was confounded by changes in the ionization state of both the buffer and the *1*. However, there may be little difference in the rate of degradation of the two ionization states of *1* (see below), and in any case the calculated species catalysis constants may be empirically useful and are included. Borate did appear to catalyze the degradation of *1*, (Table I), but this catalysis was small compared to the specific catalysis, particularly at pH values of 9.0 and greater. Furthermore, the errors due to specific catalysis made the precise determination of the borate-species catalysis constants impossible with the present data.

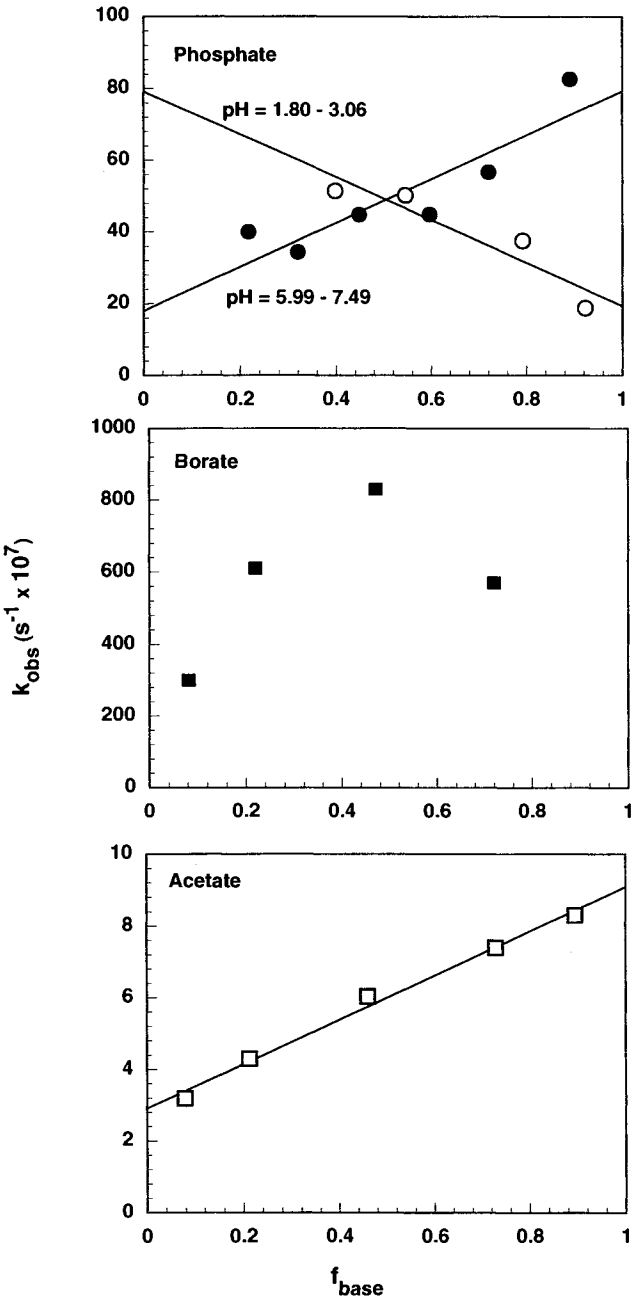

Fig. 3. Relationships between the value of k_G the buffers used to study the hydrolysis of *1* and the fraction of the basic species (f_{base}) at 36.8°C and μ = 0.5.

Table I. Catalytic rate constants for the hydrolysis of 1 at 36.8°C and μ = 0.5.

Species	Rate constant
Solvent	
H_2O (k_o, s^{-1})	3.00×10^{-8}
H^+(k_H, $M^{-1}s^{-1}$)	4.40×10^{-4}
OH^-(k_{B1}, $M^{-1}s^{-1}$)	8.00
OH^-(k_{B2}, $M^{-1}s^{-1}$)	5.70
Buffers	
H_3PO_4($M^{-1}s^{-1}$)	7.62×10^{-6}
H_2PO_4 ($M^{-1}s^{-1}$)	(a) 1.95×10^{-6}[a]
	(b) 6.51×10^{-7}[a]
HPO_4^{2-}($M^{-1}s^{-1}$)	8.42×10^{-6}
CH_3COOH($M^{-1}s^{-1}$)	2.91×10^{-7}
CH_3COO^-($M^{-1}s^{-1}$)	9.09×10^{-7}

[a] The two values of $k_{H_2PO_4^-}$ were obtained over two different pH ranges (a) 1.80–3.06 and (b) 6.25–7.49.

Phenomenological Model for the Effect of Solvent

The pH rate profile for *1* (Figure 4) at 36.8°C, μ = 0.50, and no buffer present can, by inspection, be described by:

$$k_{obs} = k_H\{H^+\} + k_o + k_{B1}\{OH^-\}f(B1) + k_{B2}\{OH^-\}f(B2) \quad (2)$$

where k_{obs} is the rate of uncatalyzed and specific acid- and base-catalyzed degradation, k_H is the specific acid catalysis constant, k_o is the rate of uncatalyzed degradation, k_{B1} is the specific base catalysis constant for the protonated *1* k_{B2} is the specific base catalysis constant for the neutral drug, $f(B1)$ is the fraction of protonated drug, and $f(B2)$ is the fraction of neutral drug. This can be transformed to:

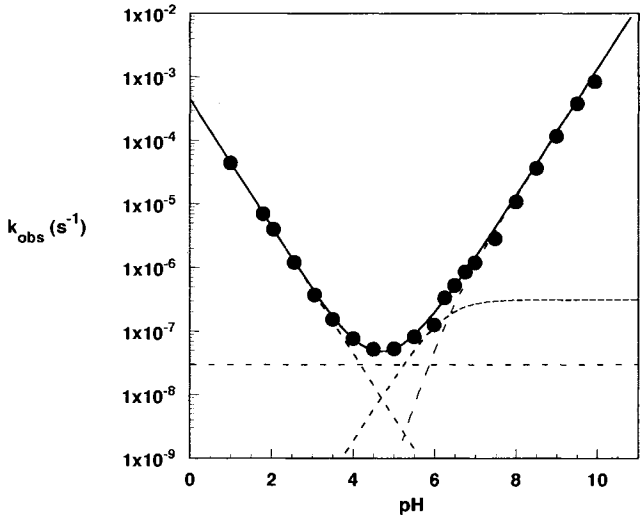

Fig. 4. k_{obs}-pH profile for the degradation of *1* at 36.8°C and μ = 0.5. The points are experimental and the lines are theoretical (Eq. 3).

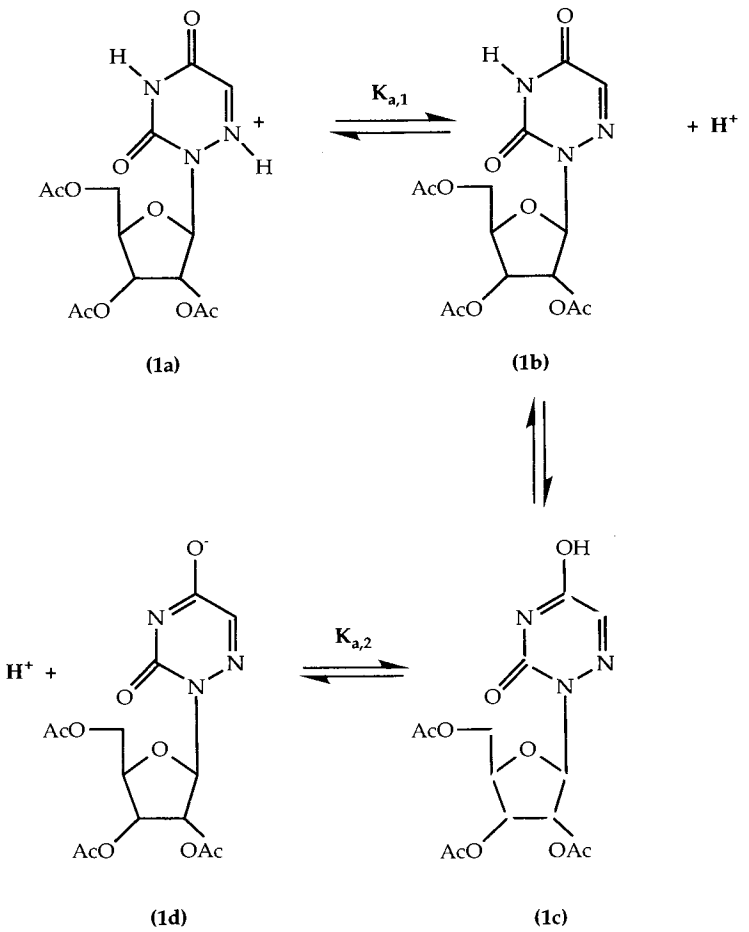

Fig. 5. Possible ionizations of 2′,3′,5′-triacetyl-6-azauridine (*1*).

$$k_{obs} = k_H\{H^+\} + k_o + \frac{k_{B1}K_w}{K_a + \{H^+\}} + \frac{k_{B2}K_wK_a}{(K_a + \{H^+\})\{H^+\}} \quad (3)$$

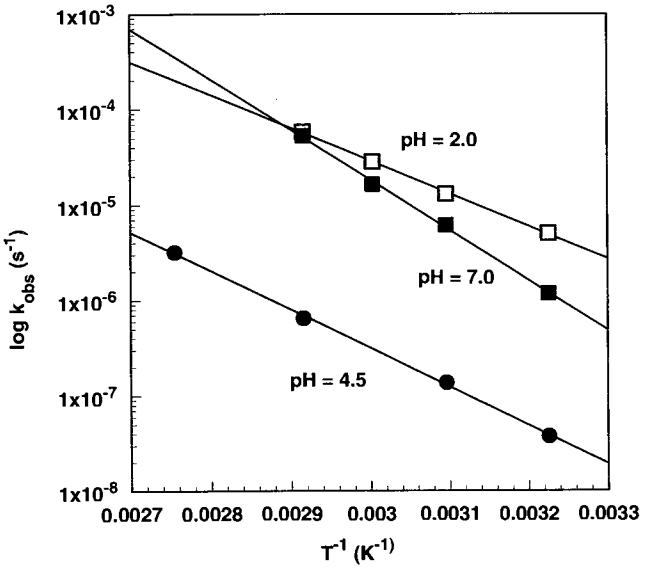

Fig. 6. Arrhenius plots for the hydrolysis of *1*, at 36.8°C, various pH values and μ = 0.5.

where K_a is the ionization constant of *1*, and K_w is the ionization constant of water.

Ionization of **1**

The title compound, *1*, was analyzed by potentiometric

Table II. Composition (as a percentage of the total peak area) of four lyophilized fractions from a preparative separation of partially degraded sample of *1*. The fractions were analyzed by gradient LC and the peak numbers are defined in Figure 2.

	Peak 3a	Peak 3b	Peak 3c	Peak 4a	Peak 4b	Peak 4c
Fraction 1*						
t = 0 h	43.8	55.6	0.0	0.0	0.0	0.0
t = 2.5 h	43.7	55.7	0.0	0.0	0.0	0.0
Fraction 2*						
t = 0	0.4	0.7	95.0	0.0	0.0	0.0
t = 2.5 h	0.4	0.7	94.9	0.0	0.0	0.0
Fraction 3						
t = 0 h	0.6	0.4	0.5	68.0	30.5	0.0
t = 2.5 h	0.5	0.5	0.5	47.1¶	51.4¶	0.0
Fraction 4						
t = 0 h	0.2	0.4	0.1	9.6	23.4	66.4
t = 2.5 h	0.2	0.4	0.1	13.5¶	19.4¶	66.4

* Also contained traces of *2*.
¶ Equilibrated solutions.

titration because the pH-profile (Eq. 3, Figure 4) suggested the influence of the ionization on the base catalyzed hydrolysis of *1*. The pK_a value for the dissociation constant of 6.15 (μ = 0.5, 36.8°C) obtained by potentiometric titration compared very favorably with the value of 6.22 obtained kinetically. The most likely site of protonation of *1* is at the N-6 position of the heterocyclic ring system. Another possibility for ionization of *1* involves deprotonation of the enolic form (*1c*) to give the anionic form *1d* (Figure 5) However, literature values for the pK_a values of analogous compounds such as uracil (10) suggest that the pK_a value arising from deprotonation at the N-3 position is greater than 10, which is outside the pH range of the present kinetic study (Figure 4).

Effect of Temperature

Linear Arrhenius plots (n = 4) at pH 2.00, 4.50, and 7.00 (Figure 6) were used to determine apparent activation energies: E_a (kcal/mol) = 16.3 at pH 2.00, 17.3 at pH 4.50, and 10.0 at pH 7.51. The activation energy of 10.0 kcal/mol at pH 7.51 has been corrected by subtracting the heat of ionization of water, which is 13.6 kcal/mol under these conditions. In these plots, the observed rate constants at 36.8°C have been corrected as follows: the uncorrected observed rate constants were measured at pH 2.06 (3.93×10^{-6} sec^{-1}), 4.51 (5.13×10^{-8} sec^{-1}), and 6.99 (1.17×10^{-6} sec^{-1}), as described in the experimental section. Then, the fitted equation for the pH rate profile was used to determine the difference in rate between pH 2.06–2.00, 4.51–4.50, and 6.99–7.00, and this difference was subtracted from the uncorrected observed rate constants to obtain the corrected observed rate constants (4.50×10^{-6} s^{-1}, 5.14×10^{-8}, and 1.20×10^{-6} s^{-1}, respectively).

Appearance of the Intermediates and the Final Product

Structural Assignments

Figure 2 shows the separation of 9 UV absorbing degradation products of *1*. The peaks corresponding to *1*, *2*, and *3* were confirmed by injection of authentic standards. Peaks *3a–c* and *4a–4c* were confirmed to be the three isomers of acetyl-6-azauridine and diacetyl-6-azauridine, respectively through MS and ^{1}H-NMR experiments, which also delineated the specific isomers corresponding to each peak.

Four lyophilized fractions (1–4) were obtained from the collected peaks of repetitive semi-preparative separations of partially degraded *1*. After reconstitution with water, the ratios of the areas of the peaks in the four fractions were determined by gradient elution LC (Table II). Those data were used as a basis for comparison with the peak ratios determined in the MS and NMR experiments. Peaks *3a–c* and *4c* were stable (less than 10% loss) for 2.5 h at room temperature. In contrast, peaks *4a* and *4c* came to equilibrium concentrations within 2.5 h, presumably through a process of acyl migration (9). Consequently, both the NMR and MS experiments were conducted immediately after reconstitution to minimize any acetyl exchange or hydrolysis.

The CI-MS spectra of the four fractions gave the following characteristic peaks: m/z 288 and 305 for the MH^+ and MNH_4^+ of the monoacetates, m/z 330 and 347 for the MH^+

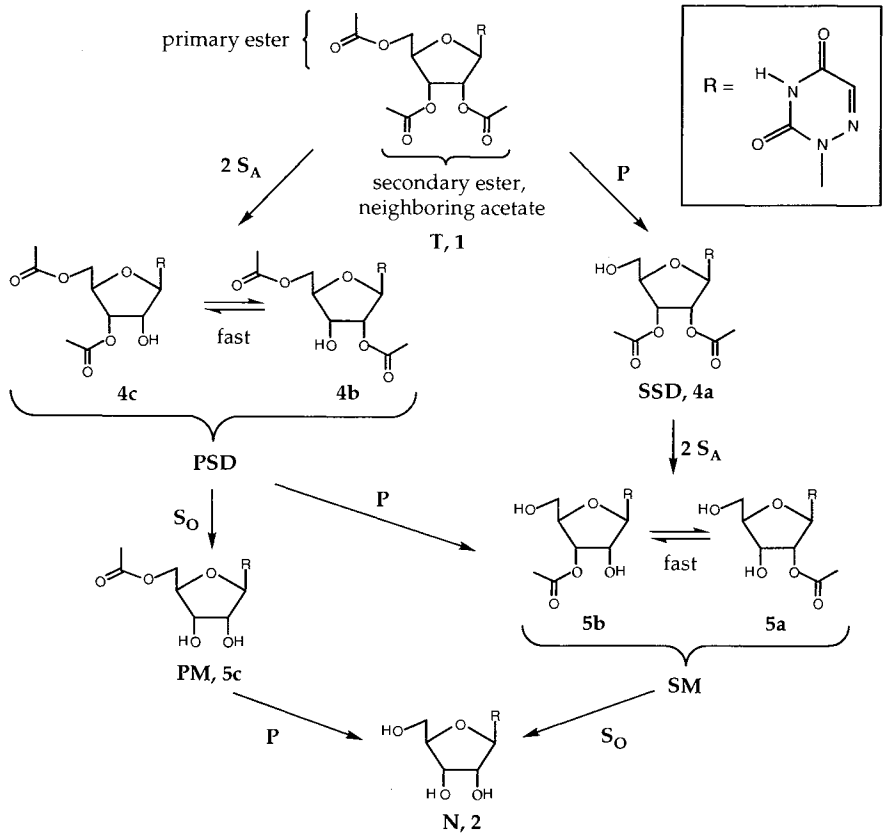

Fig. 7. Simplified kinetic scheme for the hydrolysis of 2′,3′,5′-triacetyl-6-azauridine (*1*).

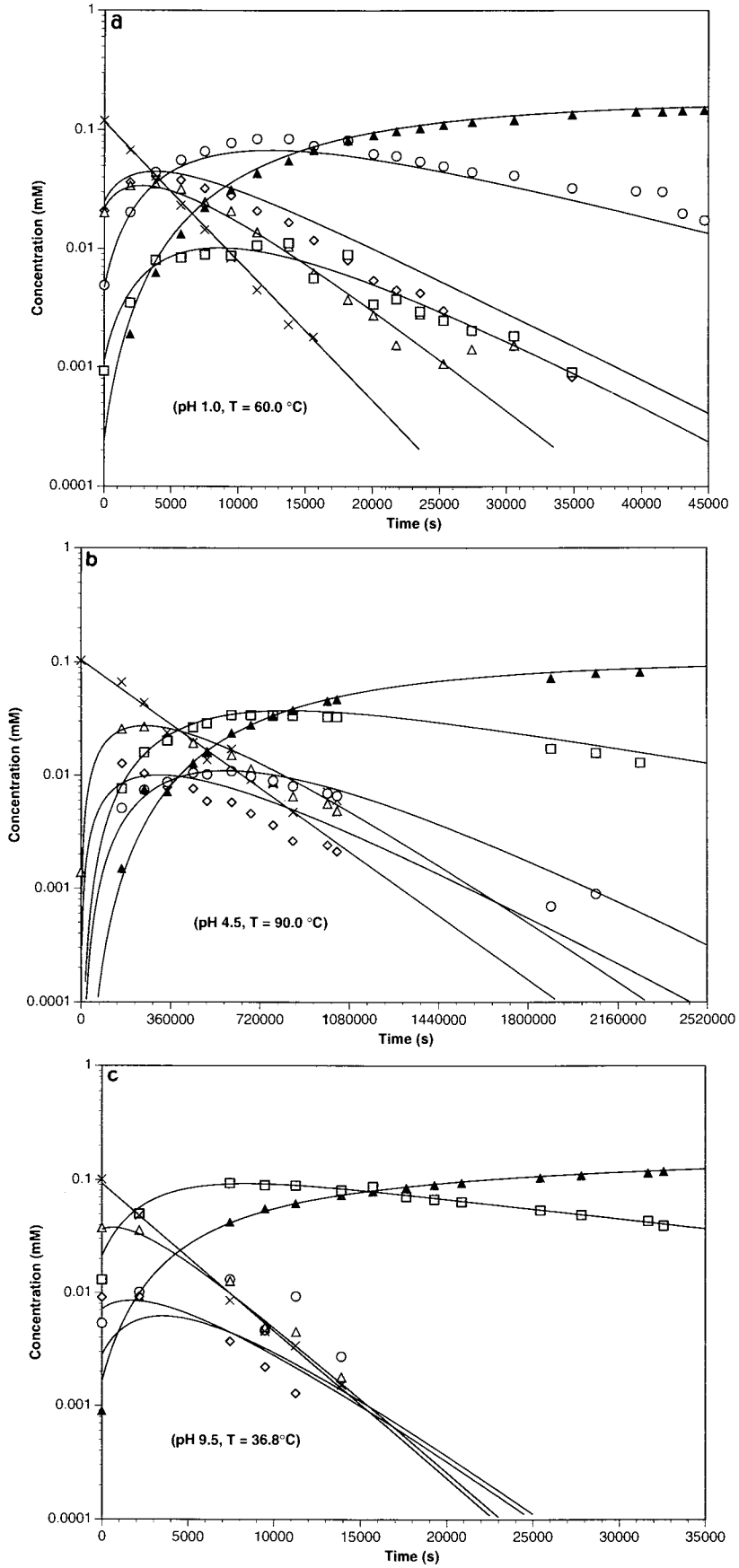

Fig. 8. Concentration-time profiles for the products of the hydrolysis of 2′,3′,5′-triacetyl-6-azauridine (*1*) at μ = 0.5 and (a) pH 1, 60.0 ± 0.1°C; (b) pH 4.5, 90.0 ± 0.1°C; and (c) pH 9.5, 36.8 ± 0.1°C. Symbols (data points are the means of two determinations, the r^2 values for the fits for Figures 8a, 8b, and 8c, respectively, are given in parentheses): X = *T*, (*1*) (r^2 values = 1.00, 0.98, 1.00); ◇ = *SSD* (*4a*) (r^2 values = 0.94, 0.76, 0.95); △ = *PSD* (*4b* + *4c*) (r^2 values = 0.99, 0.95, 0.99); ○ = *SM* (*5a* + *5b*) (r^2 values = 0.85, 0.96, 0.72); □ = *PM* (*5c*) (r^2 values = 0.90, 0.95, 0.98); ▲ = *N* (*2*) (r^2 values = 0.99, 0.99, 1.00).

Table III. Average ratio of 2′ Ac/3′ Ac/ and 2′,5′ Ac/3′,5′ Ac over the kinetic runs.

	pH 1, 60°C	pH 4.5, 90°C	pH 9.5, 36.8°C
2′ Ac/3′ Ac	0.73 ± 0.073 (RSD: 10%, n = 21)	0.68 ± 0.0093 (RSD: 1.4%, n = 11)	0.79 ± 0.21 (RSD: 26%, n = 6)
2′5′ Ac/3′5′ Ac	0.080 ± 0.13 (RSD: 16%, n = 12)	0.72 ± 0.12 (RSD: 16%, n = 12)	0.79 ± 0.14 (RSD: 18%, n = 5)

and MNH_4^+ of the diacetates and m/z 372 and 389 for the MH^+ and MNH_4^+ of the triacetate. These values confirmed that the fractions contained mixtures of mono-, di- and triacetates in proportions that were in general agreement with the LC data shown in Table II, which was assumed to be the more accurate and reliable. The peaks heights obtained by CI-MS could not be used to determine accurately the isomeric ratios because of the volatility of the components increased with the addition of each acetate group. Nevertheless, the CI-MS data confirmed the LC results that the monoacetates were the dominant species in fractions 1 and 2 and the diacetates were predominant in factions 3 and 4.

Identification of the different acetylated isomers was based on ^{1}H-NMR and COSY experiments in a manner similar to a previous study on the structurally related acetylated prodrugs of 9-β-arabinofuranylosyladenine (11). Acetylation shifted the proton directly attached to the affected carbon downfield approximately 0.8 δ, and caused a smaller shift at the adjacent protons. These shifts sometimes produced overlaps of previously well-separated peaks, but these were readily distinguished in the COSY spectra. Of the protons on the sugar moiety, the $H(1')$ was the most downfield, between 6.13 and 6.33 ppm. The $H(2')$ proton was at 5.48 ppm when the 2′ position was acetylated, shifting to 5.68 ppm when both the 2′ and 3′ positions were acetylated. The $H(3')$ proton was at 5.29–5.34 ppm, shifting to 5.50 when both the 2′ and 3′ positions were acetylated. The $H(5')$ protons were at 4.86–4.89 and nearly lost in the water peak at 4.8 δ. $H(2')$ to $H(5')$ protons not on an acetylated position were invariably upfield of the water peak. The compositions of the fractions obtained by LC analysis were in good agreement with the peak intensities obtained by NMR analysis, which thereby confirmed the positive identification of the mono- and diacetates.

Chart 1. Expressions for concentrations as functions of time

T(1): $C_T = C_0 e^{-(2S_A+P)t}$

SSD(4*a*): $C_{SSD} = C_0(e^{-2S_At} - e^{-(2S_A+P)t})$

PSD(4*b* + 4*c*): $C_{PSD} = \frac{2S_AC_0}{2S_A - S_0}(e^{-(S_0+P)t} - e^{-(2S_A+P)t})$

PM(5*c*): $C_{PM} = \frac{C_0}{2S_A - S_0}(S_0e^{-(2S_A+P)t} - 2S_Ae^{-(S_0+P)t} + (2S_A - S_0)e^{-Pt})$

SM(5*a* + 5*b*): $C_{SM} = \frac{2S_AC_0}{2S_A - S_0}(e^{-(2S_A+P)t} + e^{-S_0t} - e^{-(S_0+P)t} - e^{-2S_At})$

N(2): $C_N = C_0 - C_T - C_{SSD} - C_{PSD} - C_{PM} - C_{SM}$

t: time; C_0: initial concentration of 2′,3′,5′-triacetyl-6-azauridine; C_T: concentration of 2′,3′,5′-triacetyl-6-azauridine at time t; C_{SSD}: concentration of SSD at time t; C_{PSD}: concentration of PSD at time t; C_{PM}: concentration of PM at time t; C_{SM}: concentration of SM at time t; C_N: concentration of N at time t (see Figure 8 for further information).

Kinetic Analysis

The serial and parallel deacetylation reactions of *1* through the three diacetate esters (*4a–c*) and three monoacetate esters (*5a–c*) present a complex kinetic picture, requiring in principle 16 rate constants even if all deacetylations are considered irreversible (Figure 7). In order to fit the concentration-time profiles of Figures 8a–c, a simplification of the general scheme was sought. First, it was reasoned that the 5′-deacetylation reactions of all isomers might have nearly the same rate constant, characteristic of primary alkyl acetates, which was designated P. Second, it was considered that 2′ and 3′ deacetylation reactions might all occur with a common rate constant characteristic of secondary alkyl acetates, which was designated S. Third, it was considered the hypothesis that migration of an acetyl group between the 2′- and 3′-hydroxyl groups of *4b*, *4c*, *5a* and *5b* might be much faster than the deacetylation reactions so that the two pools {*4b* + *4c*} and {*5a* + *5b*} could each be considered in rapid internal equilibrium.

To test the rapid-equilibrium hypothesis, the ratio of 2′-OAc/3′-OAc esters was calculated at each time point for each of the pools. If the pools were at equilibrium throughout a kinetic run, then this ratio should have been constant throughout the run. The ratios are shown in Table III. They exhibited no systematic time dependence and, within an error of up to about 25%, were essentially constant. In fact, the ratio is constant at around 0.7–0.8 for all pH values and temperatures studied. It was concluded that these pools are at equilibrium on the time scale of the experiments (hours) and that the equilibrium constant for conversion of 2′-OAc to 3′-OAc was 0.7–0.8, independent of pH (which is expected) and temperature (which is reasonable).

Assuming then that the pools are in equilibrium, the kinetic system can be simplified (Figure 7) to (a) conversion of the triacetate T (*1*) to the pool PSD (primary, secondary diacetates *4b* and *4c*) and the secondary-secondary diacetate SSD (*4a*); (b) conversion of PSD to the primary monoacetate

Table IV. Rate constants (s^{-1}) chosen to obtain the fits shown in Figures 8a–c.

	pH 1.0, 60.0°C	pH 4.5, 90.0°C	pH 9.5, 36.8°C
$10^7 P$	1400	8.3	400
$10^7 S_A$	650	14	1300
$10^7 S_O$	700	33	4900

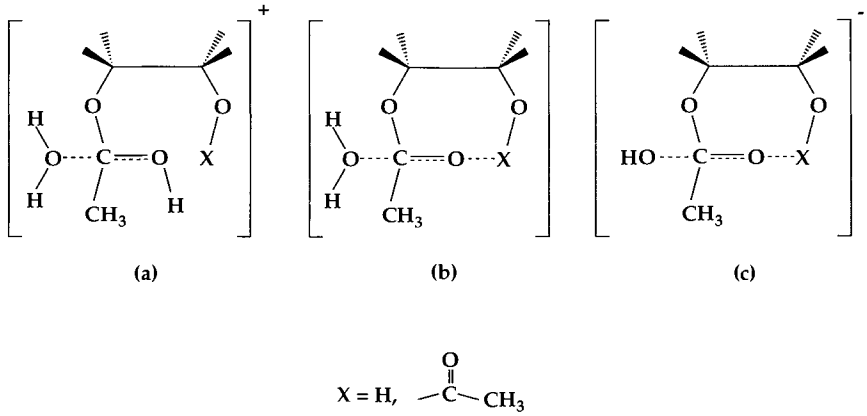

Fig. 9. Transition-state structures for (a) acidic, (b) neutral, and (c) basic hydrolysis of 2',3'-diacetates and 2'- or 3'-monoacetates, illustrating the lack of neighboring group electrophilic assistance in acidic solution and its presence in neutral and basic solution.

PM (*5c*) and the pool of secondary monoacetates SM (5a + 5b), along with conversion of SSD to SM; (c) conversion of PM and SM to the nucleoside N2. Initial attempts to fit the data to this simplified scheme, employing a single rate constant P for deacetylation of all 5'-acetates and a single rate constant S for deacetylation of all 2' and 3' acetates gave an inadequate account of the data. This result suggested that in place of S, two rate constants (S_O for deacetylation of a secondary center adjacent to a secondary OH group, and S_A for deacetylation adjacent to an OAc group) be employed. This modified scheme led then to the assignment of rate constants depicted in Figure 7. The time-dependencies for T, PSD, SSD, PM, and SM can then be obtained by integration of the differential equations (Chart 1) and the concentration of N obtained from the material balance.

Values of the rate constants were adjusted by a combination of least-squares and manual fitting to obtain the curves shown in Figures 8a–c. These figures confirm that the concentration profiles for all compounds under the three sets of reaction conditions could be described by a simple kinetic model with only three adjustable parameters, the rate constants P, S_O, and S_A. The quality of the final fits shown in the figures can be judged by the correlation coefficients presented in Figures 8a–c. The model accounts for 72 to nearly 100% of the total variance for all of the 18 concentration-time profiles, and accounts for 95% or more of the variance in 13 of the 18 cases.

The values of the rate constants P, S_O, and S_A are shown in Table IV. Since the three sets of reaction conditions employed involve the simultaneous variation of pH and temperature, no significant quantitative conclusions can be reached. It is notable that in acidic solution, the primary acetates react more rapidly than the secondary acetates, while in neutral and basic solution, the opposite is true. Steric considerations suggest that the near-tetrahedral transition states for hydrolysis should form more readily with esters of the smaller primary alkyl group than with esters of the larger secondary alkyl group, as seen in acidic solution. The faster hydrolysis of the secondary esters in neutral and basic solution may derive from the fact that both kinds of secondary ester are located adjacent and *cis* to either a hydroxyl group (rate constant S_O) or an acetyl group (rate constant S_A). Both neighboring groups can accelerate attack at the adjacent ester center by electrophilic assistance (Figure 9); the hydroxyl group can donate a hydrogen bond to the carbonyl oxygen that is becoming negative as water attacks (neutral solution) or as hydroxide ion attacks (basic solution). This effect is absent in acidic hydrolysis, where the catalytic proton has already bonded to the carbonyl oxygen before attack by water, precluding any electrophilic assistance from a neighboring hydroxyl or acetyl group. Presumably, therefore, the steric is seen unopposed in acidic solution, while the electrophilic effect more than cancels the steric effect in neutral and especially in basic solution.

CONCLUSIONS

At 36.8°C, the pH-rate profile of *1* in water was adequately described by a four-term rate equation and the following apparent activation energies for the loss of *1* were obtained: 16.3 kcal/mol at pH 2.00, 17.3 kcal at pH 4.50, and 23.6 kcal/mol at pH 7.00. A simplified kinetic scheme was developed to describe the time course of *1*, the intermediates and final product involving (a) the conversion of *1* to the pool PSD (primary and secondary acetates); (b) conversion of PSD to the primary monoacetate PM and the pool of secondary monoacetates SM along with conversion of SSD to SM; and (c) conversion of PM and SM the nucleoside (6-azauridine). The data could be fitted to this simplified scheme with only three rate constants, *i.e.*, a single rate constant P for the deacetylation of all 5'-acetates and two rate constants S_O for the deacetylation of a secondary center adjacent to a secondary OH group and S_A for the deacetylation adjacent to an OAC group.

ACKNOWLEDGMENTS

This work was supported by a training grant from the National Cancer Institute (CA 09242), a Merit Review grant from the Veterans Administration, and a grant from Sterling-Winthrop. The authors are grateful to Dr. Todd Williams of the University of Kansas Mass Spectrometry Laboratory for providing the CI spectra and the interpretation of the results. Parts of this study have been previously published in the MS Thesis of Michael A. Mummert (University of Kansas) and

parts were presented at the Eighth (Orlando) and Ninth (San Diego) Annual Meetings of the American Association of Pharmaceutical Scientists.

REFERENCES

1. A. D. Welch, R. E. Handschumacher, and J.J. Jaffe. Studies on the pharmacology of 6-azauracil. *J. Pharm. Exp. Ther.* **129**:262–269 (1960).
2. J. Koda, In A. C. Sartorelli and D. G. Johns, (Eds.), *Handbook of Experimental Pharmacology*, 38 Springer Verlag, Berlin 1975, pp. 348–372.
3. C. H. Doolittle, C. J. McDonald, and P. Calabresi. Pharmacological Studies of Neurotoxicity in Patients with Psoriasis Treated with Azaribine, Utilizing High Pressure Liquid Chromatography. *J. Lab. Clin. Med.* **90**:773–785 (1977).
4. A. D. Welch, R. E. Handschumacher, S. E. Finch, and J. J. Jaffe. A Synopsis of Recent Investigations of 6-Azauridine (NSC-32074). *Cancer Chemother. Rep.* **39**:39–46 (1960).
5. F. Sorm and J. Vesely. Potentiation of the Cancerostatic Effect of 6-Azauridine and 6-Azacytidine with 5-Bis-(2-chloroethyl)-aminomethyluracil. *Experientia* **17**:355 (1961).
6. W. Drell and A. D. Welch. Azaribine homocystinemia-thrombosis in historical perspective. *Pharmacol. Ther.* **41**:195 (1989).
7. M. Slavik, K. J. Smith, and O. Blanc. Decrease of Serum Pyridoxal Phosphate Levels and Homocystinemia after Administration of 6-Azauridine Triacetate and Their Prevention by Administration of Pyridoxime. *Biochem. Pharmacol.* **31**:4089–4092 (1982).
8. R. E. Handschumacherm, P. Calabresi, A. D. Welsh, V. Bono, H. Fallon, and E. Frei. Summary of Current Information on 6-Azauridine. *Cancer Chemother. Rep.* **21**:211–18 (1962).
9. A. Albert and E. P. Sergeant. *The Determination of Ionization Constant*. Chapman and Hall, London, 1–40 (1971).
10. R. M. Izatt, J. J. Christensen, and J. H. Rytting. *Chem Rev.* **71**:439–481 (1971).
11. B. Anderson, M. Fung, S. Kumar, and D. Baker. Hydrolysis and Solvent Dependent 2′–5′ and 3′–5′ Acyl Migration in Prodrugs of 9-β-Arabinofuranylosyladenine. *J. Pharm. Sci.* 74:8 825–830 (1985).